



## Adsorption characteristic of U(VI) ion onto thermally activated bentonite

S. Aytas<sup>a</sup>, M. Yurtlu<sup>a</sup>, R. Donat<sup>b,\*</sup>

<sup>a</sup> Ege University, Institute of Nuclear Sciences, 35100 Bornova-Izmir, Turkey

<sup>b</sup> Pamukkale University, Faculty of Sciences and Arts, Department of Chemistry, 20070 Denizli, Turkey

### ARTICLE INFO

#### Article history:

Received 20 February 2009

Received in revised form 14 July 2009

Accepted 14 July 2009

Available online 22 July 2009

#### Keywords:

Bentonite

Thermal treatment

Calcination

Adsorption

Uranium

### ABSTRACT

In this study, the effect of pH, contact time, temperature, and initial metal concentration on U(VI) adsorption on thermally activated bentonite (TAB) was investigated. Graphical correlation of various adsorption isotherm models like, Freundlich, and Dubinin–Radushkevich have been carried out for TAB. Various thermodynamic parameters, such as, Gibb's free energy, entropy and enthalpy of the on-going adsorption process have been calculated. In order to reveal the adsorptive characteristic of bentonite samples, surface area, FT-IR, and DTA-TG spectra analyses were carried out. The results show that TAB samples can be an alternative low cost adsorbent for removing U(VI) ions from aqueous solutions.

© 2009 Elsevier B.V. All rights reserved.

### 1. Introduction

Adsorption of metal ions onto clay minerals has been studied extensively because both metal ions and clays are common components in nature and also because a knowledge of the adsorption process could aid in the environmental remediation of water that is polluted by heavy metal ions [1]. These clays are chosen to avoid pollutant release into the environment owing to their high specific surface areas, low cost and ubiquitous presence in most soils [2]. Economical and eco-friendly method, adsorption technique has been used widely to remove heavy metal ions from aqueous solutions. In the recent years, many kinds of natural clay minerals such as, diatomite [3], illite [4], bentonite [5], palygorskite [6], attapulgite [7], and sepiolite [8] have been used to remove heavy metal ions from wastewater. In these clay minerals, bentonite is considered as main candidate in the decontamination and treatment of detrimental metal ions due to its large specific surface area and high sorption capacity.

Bentonites are highly valued for their sorptive properties, which stem from their high surface area and their tendency to absorb water in the interlayer sites [9]. Bentonite as an adsorbent for the removal  $UO_2^{2+}$  ions and other metal ions under estuarine and seawater conditions has been reported earlier [10,11]. Several studies have been carried out to identify and differentiate the sorption sites of uranyl species on phyllosilicate minerals under different chemical conditions. Dent et al. [12] proposed the formation of an

outersphere uranyl sorption complex onto montmorillonite by an ion-exchange mechanism and discussed the possibility of exchange reactions of uranyl carbonate complexes in the interlayer of montmorillonite at pH 5.

An important characteristic that clay minerals are able to provide in such applications is adequate particle dispersion, which is necessary to obtain a uniform and stable system. Under certain conditions the clay particles may become aggregated, which leads to the variation of important properties required for a particular function. This is important for many industrial applications of clay minerals [13].

Bentonites may be subjected to high temperatures when used in these applications and their physicochemical properties may change as a result of thermal treatment [14]. Dehydration and dehydroxylation processes during calcination of clay minerals [15] can be accompanied by movements of octahedral cations within the octahedral sheet [16]. Besides these structural changes, calcination also changes the textural properties and influences the dispersibility in water. Sorption onto bentonite will play an important role in retarding the migration of many radionuclides from a waste repository.

In this study, the ability of TAB to adsorb uranium in solution and to desorb uranium from TAB was shown as a function of some experimental parameters. Adsorption isotherms have been analyzed in terms of Freundlich, and Dubinin–Radushkevich (D–R) equations. Thermodynamic parameters such as enthalpy of adsorption ( $\Delta H$ ), free energy change ( $\Delta G$ ), entropy change ( $\Delta S$ ), and mean free energy of adsorption ( $E$ ) have been calculated and interpreted. Optimal adsorption conditions are reported. The sorption process based on TAB represents a

\* Corresponding author. Tel.: +90 258 2963602; fax: +90 258 2963535.

E-mail address: [rdonat@pau.edu.tr](mailto:rdonat@pau.edu.tr) (R. Donat).

possible alternative to the conventional uranium separation processes.

## 2. Materials and methods

### 2.1. Materials

In this study, grey bentonite also known as Turkish merchant obtained from Karakaya A.S. Mineral Company, Cankiri-Turkey was used as an adsorbent. Bentonite mineral was grounded and sieved to give 125  $\mu\text{m}$  size using ASTM Standard sieves. The minerals were washed with deionised water and then dried.

### 2.2. Characterization methods

Natural bentonite was characterized by X-ray fluorescence spectrophotometry (XRF) and chemical analysis. Chemical composition of natural bentonite sample was found out by standard wet chemical analysis along with instrumental methods [17].  $\text{Al}_2\text{O}_3$ ,  $\text{Fe}_2\text{O}_3$ ,  $\text{CaO}$  and  $\text{MgO}$  were analyzed with titrimetric and  $\text{SiO}_2$  was analyzed with gravimetric method.  $\text{Na}_2\text{O}$  and  $\text{K}_2\text{O}$  were found out by flame photometry. Specific surface area of natural bentonite was measured by  $\text{N}_2$ , BET method:  $S_B$ : 43.61  $\text{m}^2/\text{g}$ .

The Fourier transform infrared (FT-IR) spectra using KBr pressed disk technique were conducted by Perkin Elmer Spectrum BX Infrared spectrometer. Natural bentonite and KBr were weighted and then were grounded in an agate mortar for 10 min prior to pellet making. The spectra were collected for each measurement over the spectral range of 400–4000  $\text{cm}^{-1}$ .

All of the thermogravimetry (TG), differential thermogravimetry (DTG), and differential thermal analysis (DTA) curves were obtained simultaneously by using a Shimadzu DTG-60H Thermal Analyzer. The measurements were carried out in flowing nitrogen atmosphere with a flow rate of 50  $\text{mL}\cdot\text{min}^{-1}$  and the between temperature range of 25 and 1000  $^\circ\text{C}$  in aluminium crucible. The heating rates were 8, 6, 4  $^\circ\text{C}\cdot\text{min}^{-1}$  and the sample masses were in the range of 10–12 mg. Highly sintered  $\text{Al}_2\text{O}_3$  was used as the reference material.

### 2.3. Adsorbent preparation

Dehydration of bentonites provides a simple possibility to modify the adsorption properties of these clay minerals. Sample of the bentonite was heated from 100 to 1000  $^\circ\text{C}$  for 1 h. The hot samples were cooled down to room temperature over silicagel.

### 2.4. Reagents

All reagents used were of analytical purity. Synthetic solutions were prepared from concentrated stock solutions (Merck). A stock solution of uranium was prepared by dissolving required amount of  $\text{UO}_2(\text{NO}_3)_2\cdot 6\text{H}_2\text{O}$  (Merck) in pure distilled water. The stock solution was diluted to prepare working solutions. The buffer solutions (pH 4, 7 and 9) were used to calibrate the pH meter. The pH of each test solution was adjusted to the required value with diluted  $\text{HNO}_3$  and  $\text{Na}_2\text{CO}_3$  solutions at the start of the experiment. Reagent blank were run for every sample solution.

### 2.5. Instrumentation

U(VI) concentrations were determined by UV-Vis Spectrophotometer (Shimadzu UV-Vis 1601 Model Spectrophotometer). The adsorption/desorption experiments have been studied by batch technique using a thermostated shaker bath GFL-1083 Model. The pH of all solution was measured with an Hanna Instrument 8521 Model pH meter. A Hettich Zentrifugen Rotofix 32 Model digital

centrifuge was used to centrifuge the samples. A Corning model flame photometer was used for the determination of Na and K elements in bentonite sample. A Electro-Mag M420 Model oven was used to dry the samples.

### 2.6. Determination of the uranium uptake capacity of bentonite

0.125 g bentonite and 0.01 M U(VI) aqueous solution were shaken for 24 h at 30  $^\circ\text{C}$ . The uptake capacity of bentonite was determined spectrophotometrically using salicylic acid as complexing agent at 468 nm against reagent blank [18]. The amount of uranium uptake ( $\text{mmole}\cdot\text{g}^{-1}$  adsorbent or  $\text{mg}/\text{g}$  adsorbent) is calculated from the differences of the uranium concentration in the substrate before and after uptake.

### 2.7. Batch adsorption experiments

All the sorption experiments were performed using the TAB. 0.1 g TAB was suspended in 10 mL of  $[\text{UO}_2(\text{NO}_3)_2\cdot 6\text{H}_2\text{O}]$  uranium solution in a polyethylene (PE) flask at selected pH. The flasks were shaken at different temperatures for various mixing times. The solution was separated from the solids by centrifugation (5 min at 3000 rpm). Then the residual U(VI) ions in aqueous solution were determined spectrophotometrically using TOPO-DBM (tri-octyl phosphine oxide and di-benzoyl methane) method at 405 nm using spectrophotometer [19].

### 2.8. Calculation

The adsorption capacity of U(VI) ions adsorbed per gram adsorbent ( $\text{mg}/\text{g}$ ) was calculated using the equation:

$$q_e = (c_o - c_e) \frac{V}{m} \quad (1)$$

The amount of adsorbed U(VI) was calculated from the difference of the uranium concentration in aqueous solution before and after adsorption. The adsorption percentage of U(VI) ions was calculated by the difference of initial and final concentration using the equation expressed as follows:

$$R = \frac{(C_o - C_e) \times 100}{C_o} \quad (2)$$

where  $q_e$  is the equilibrium concentration of U(VI) on the adsorbent ( $\text{mg}/\text{g}$ ),  $C_o$  the initial concentration of the U(VI) solution ( $\text{mg}/\text{L}$ ),  $C_e$  the equilibrium concentration of the U(VI) solution ( $\text{mg}/\text{L}$ ),  $m$  the mass of adsorbent (g),  $V$  the volume of U (VI) solution,  $R$  the retention of U(VI) in % of the added amount.

## 3. Results and discussion

### 3.1. Material characterization

Chemical analysis of bentonite is presented in Table 1. This study showed that natural bentonite contained a complement of exchangeable sodium, potassium and calcium ions. The (Na + K)/Ca is ratio 1.11. Low-silica members are enriched with calcium, whereas high-silica montmorillonite are enriched with potassium, sodium and magnesium. The uranium uptake capacity of the bentonite was 27  $\text{mg}\cdot\text{UO}_2^{2+}/\text{g}$ . The uptake experiment shows that bentonite uptakes considerable amount of uranium from solution.

FT-IR studies of natural bentonite adsorbent help in the identification of various forms of the minerals present in the clay. The adsorbent was characterized by FT-IR spectroscopic analysis before and after the adsorption process (Fig. 1). Before U(VI) adsorption, the broad bands at 3629.54 and 3447.72  $\text{cm}^{-1}$  are due to the O–H stretching vibration of the silanol (Si–OH) groups from the solid

**Table 1**  
The chemical composition of the natural bentonite.

Component	w/w (%)
SiO <sub>2</sub>	58.18
Al <sub>2</sub> O <sub>3</sub>	14.53
Fe <sub>2</sub> O <sub>3</sub>	5.78
CaO	3.98
MgO	3.03
Na <sub>2</sub> O	2.54
K <sub>2</sub> O	1.71
Loi <sup>a</sup>	9.90

<sup>a</sup> Loi: loss of ignition.

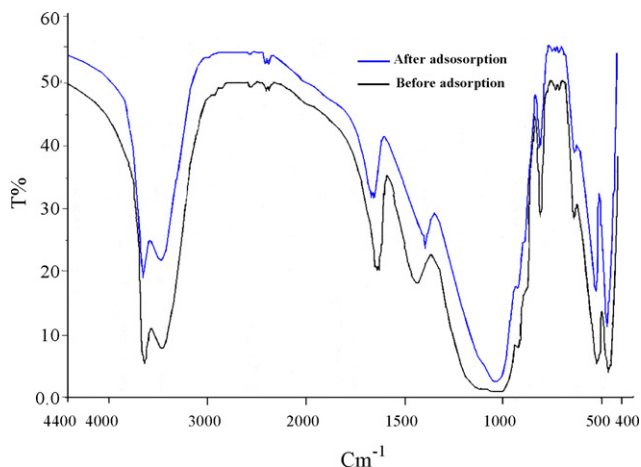


**Fig. 1.** The FT-IR spectra of bentonite before and after U(VI) adsorption.

and HO–H vibration of the water molecules adsorbed on the silicate surface. The band at  $1636.36\text{ cm}^{-1}$  reflects the bending HO–H bond of water molecules, which is retained in the silicate matrix. The strong band at  $1030.16\text{ cm}^{-1}$  represents the Si–O–Si groups of the tetrahedral sheet. The bands at  $527.48$  and  $466.06\text{ cm}^{-1}$  are due to the deformation and bending modes of the Si–O bond [20]. A sharp band at  $796.72\text{ cm}^{-1}$  confirms the presence of quartz admixture in the sample. The bands corresponding to AlAlOH, AlFeOH and AlMgOH bending vibrations are observed at  $916$ ,  $887$  and  $847\text{ cm}^{-1}$ , respectively. After the adsorption of U(VI) the Si–O–Si bond of the adsorbent has shifted from  $1030.16$  to  $1040.77\text{ cm}^{-1}$  and the deformation and bending bands of the Si–O bond at  $527.48$  and  $466.06\text{ cm}^{-1}$  have also shifted to  $524.37$  and  $469.34\text{ cm}^{-1}$ . The stretching vibration of AlAlOH, AlFeOH and AlMgOH at  $916\text{ cm}^{-1}$  has shifted to  $919\text{ cm}^{-1}$ . The O–H stretching vibration band of the silanol group (Si–OH) at  $3629.54$  and  $3447.72\text{ cm}^{-1}$  has shifted to  $3629.79$  and  $3447.97\text{ cm}^{-1}$ , respectively.

Result from thermal analysis is reported in Fig. 2. The TG curve of the original sample shows three main steps of weight loss. In the first step ( $T < 200^\circ\text{C}$ ) a weight loss (about 7.61%) corresponding to both adsorbed and interlayer water loss takes place. After this step, the TG curve shows a slight gradual decrease (about 3.30%) in the range  $162$ – $562^\circ\text{C}$ , which is attributed to the water loss of bentonite. Finally, a third main loss occurs at temperatures in the range  $522$ – $700^\circ\text{C}$ , where the TG curve displays a step weight loss (about 3.61%) related to the release of structural OH of natural bentonite. The dehydroxylation temperature of about  $665^\circ\text{C}$  (Fig. 2) is in agreement with the classical range of dehydroxylation temperature ( $600$ – $700^\circ\text{C}$ ) observed by various authors for cis vacant montmorillonites [21]. Natural bentonite sample loses the structural OH<sup>−</sup> in two different steps: (i) Continuously at temperatures well below  $600^\circ\text{C}$  from a defective montmorillonite structure, and

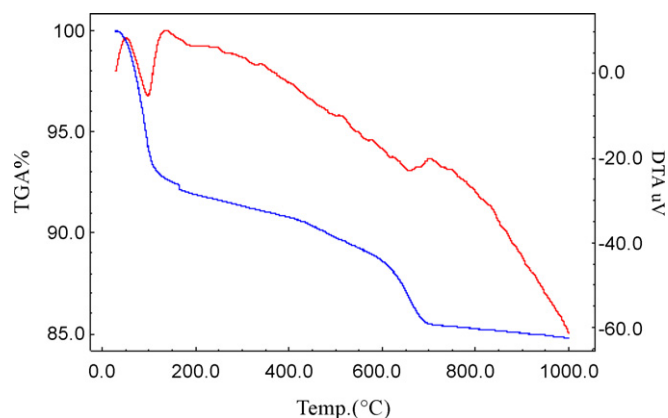


**Fig. 2.** DTA and TG curves of natural bentonite.

(ii) in the range  $600$ – $700^\circ\text{C}$  with a similar trend of undefective montmorillonite.

### 3.2. Effect of calcination temperature

Natural aluminosilicates are polymineral substances that differ in composition, content of clay minerals, specifics of their crystalline structure and presence of impurities. Aluminosilicate materials are used in both natural and modified form for treatment of aqueous solutions and wastewaters. The removal of heavy metal ions by clay minerals (montmorillonite, illite, kaolinite) has been the subject of a number of investigations [22]. The thermal modification of aluminosilicates changes their composition, structure and sorption ability. In order to determine the optimum conditions for thermal treatment, the influence of temperature ( $150$ – $900^\circ\text{C}$ ) on the change of structure, adsorption and physicochemical properties of different kinds of clays were investigated [23].

Fig. 3 illustrates the decrease in the mass of the bentonite samples, which were heated for 1 h at different temperatures, recorded as the loss on ignition (Loi). The loss in weight of the bentonite sample on heating was attributed to the loss of moisture. Fig. 3 was characterized by a definite change in curvature, beginning at about  $100^\circ\text{C}$ . Above  $550^\circ\text{C}$  the amount of water removed changed only slightly with increase of temperature. The break in the curve at  $300^\circ\text{C}$  corresponds to a water loss of approximately 3.25 percent in the original sample, respectively. The destroying of the crystalline

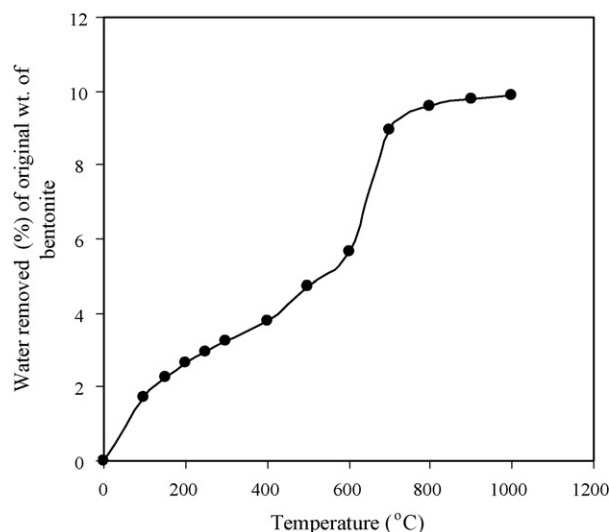


**Fig. 3.** Dehydration curves for the natural bentonite.

lattice (amorphization) of hydromicaceous clays (illite) is observed at temperatures from 550 to 650 °C [24]. The temperatures of amorphization of various minerals depend on the size of the particles and on the degree of crystallization. The data of the thermal modification concern mainly clays and show that the structural changes observed with the increasing of temperature are an individual and specific feature for clays similar in their chemical and mineralogical composition. In the preliminary investigation it was found out that a correlation between the temperature mode of treatment of four Bulgarian clay marls and their removal ability concerning heavy metal ions from water solutions exists [25].

Chorom and Rengasamy (1996) suggested that, although the migration of larger cations ( $\text{Na}^+$ ,  $\text{K}^+$  and  $\text{Ca}^{2+}$ ) into clay lattices is not possible, thermal energy at temperatures around 400 °C increases the covalency of their bonding to the clay mineral surfaces [26]. The thermal reactions of clay minerals are well established: dehydration occurs first, then dehydroxylation before, finally, structural breakdown and the formation of new minerals such as mullite ( $\text{Al}_6\text{Si}_2\text{O}_{13}$ ), cristobalite ( $\text{SiO}_2$ ) and feldspars (Na, K or Ca aluminosilicates) at temperatures above around 900 °C [27].

According to many other investigators, these values correspond to the water formed in the decomposition of hydroxyl groups in the bentonite. Therefore, the activated product on this basis would contain only two-thirds of the constitutional hydroxyl groups contained in the original bentonite.

### 3.3. Effect of calcination temperature on the adsorption of U(VI) onto TAB

The sorption of U(VI) ions has been investigated onto TAB as a function of calcinations temperature in the range of 100–500 °C. Calcination of the bentonite at 100–500 °C decreased the specific surface area because desorption of hydration and interlayer water closes the interlayer spaces and causes a denser packing of the particles. The adsorption properties of bentonites change when the samples are calcined at 350–550 °C, i.e. at conditions that the layer structure is retained. Fig. 4 has shown the adsorption of U(VI) ions onto TAB sample. When bentonite was calcinated at 400 °C, the adsorptive capacity is highest but decreases when above 400 °C. This is because that the rise of temperature breaks the crystal structure and decreases the specific surface area and adsorbability.

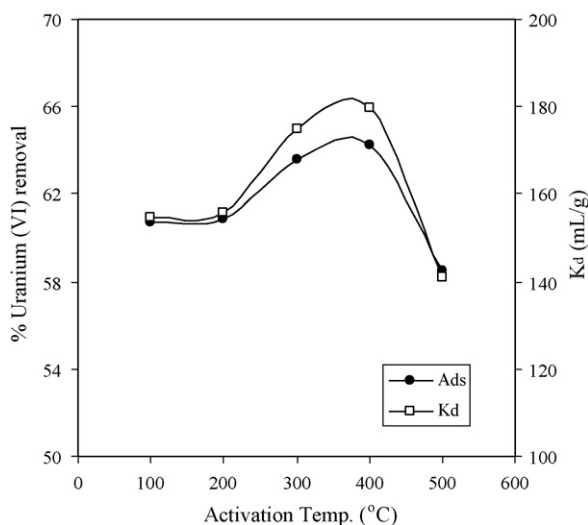


Fig. 4. The effect of activation temperature (conditions: adsorbate conc., 75 mg/L; pH, 3.0; adsorbent dose, 0.1 g; contact time, 3 h; temp., 30 °C; particle size of TAB, 125 μm).

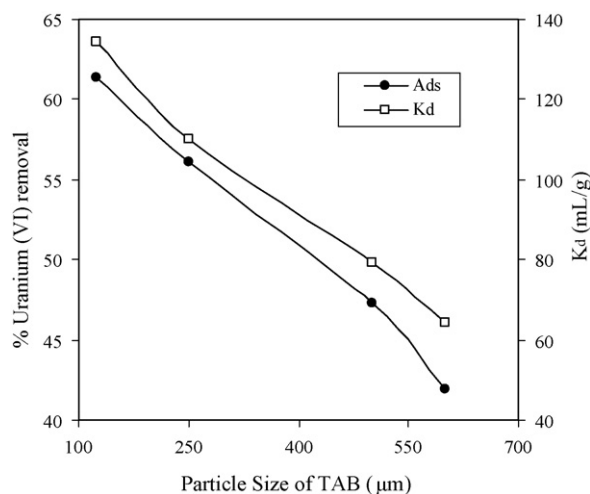


Fig. 5. Effect of particle size of TAB (conditions: adsorbate conc., 75 mg/L; pH, 3.0; adsorbent dose, 0.1 g; contact time, 3 h; temp., 30 °C; calcination temp., 400 °C).

The dehydration and dehydroxylation processes during calcinations of clay minerals can be accompanied by movements of octahedral cations within the octahedral sheet [28]. Besides these structural changes, calcination also changes the textural properties and influences the dispersibility in water. These changes can be used to enhance uranium ions adsorption. Therefore, thermally calcinations temperature 400 °C was selected for further adsorption experiments.

### 3.4. Effect of particle size of TAB

The pore properties (i.e., surface area and total pore volume) play a significant role in determining adsorption capacity based on the results of the adsorption equilibrium and adsorption kinetics experiments. The result of  $\text{UO}_2^{2+}$  adsorption on the amount of TAB is shown in Fig. 5. The concentration of  $\text{UO}_2^{2+}$ , pH, temperature and shaking time were fixed at 75 mg/L, 3.0, 30 °C and 3 h, respectively, while the particle size of TAB was varied from 600 to 125 μm. The percentage adsorption and distribution coefficient ( $K_d$ ) decrease while increasing the size of TAB up to 600 μm. This is because of increasing the external surface area TAB particle, and as a result, more active sites are exposed to  $\text{UO}_2^{2+}$  ions. Therefore, the size of TAB (125 μm) adsorbent was selected for further adsorption experiments.

### 3.5. Effect of initial pH

The pH of the aqueous solution is an important variable for the adsorption of metals on the adsorbents. The effect of the pH on the U(VI) adsorption by TAB was studied in the pH region between 2.0 and 9.0, where the material exhibits chemical stability. For that purpose, the pH values of uranium solutions were adjusted a range of 2.0–9.0 prior to the experiments. Buffers of different chemical compositions were used to calibrate pH meter. As seen in Fig. 6, the adsorption of uranium increases from 31.03 to 64.75% with an increase in pH of the solution from 2.0 to 4.0 and then decreases to 59.42% at pH 6.0.

The TAB has a maximum sorption at pH 9.0. The high adsorption levels for the TAB between pH 3 and 4 indicate that a high affinity for  $\text{UO}_2^{2+}$  predominant in this pH region. At higher pH values, the speciation of U(VI) is dominated by a series of strong aqueous carbonate complexes which increase the solubility of uranium at these environmental conditions. In the pH range of 7–10, the soluble carbonate complexes of  $\text{UO}_2^{2+}$  are the dominant



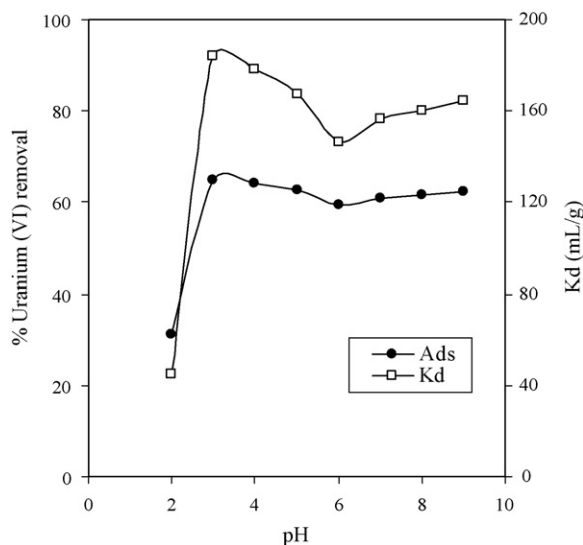


**Fig. 6.** The effect of pH (conditions: adsorbate conc., 75 mg/L; adsorbent dose, 0.1 g; contact time, 2 h; temp., 30 °C; calcination temp., 400 °C; particle size of TAB, 125 μm).

anion species— $\text{UO}_2(\text{CO}_3)_3^{2-}$  and  $\text{UO}_2(\text{CO}_3)_3^{4-}$ . These two complexes exist in various ratios depending on the pH of the solution [29]. At low pH, the uranyl exists primarily as a mononuclear, aqueous ionic species, and outersphere complexation is the principal method of adsorption. For uranium adsorption onto montmorillonite in solutions of low pH and low ionic strength, cation exchange at negatively charged surface sites has been shown to be an important mechanism [30]. Montmorillonite can adsorb heavy metals via two different mechanisms: (1) cation exchange in the interlayers resulting from the interactions between ions and negative permanent charge, (2) formation of inner-sphere complexes through Si–O<sup>−</sup> and Al–O<sup>−</sup> groups at the clay particle edges [31]. Both mechanisms are pH dependent because in acid conditions (pH < 4) most silanol and aluminol groups are protonated; therefore, in particular for the latter, an acidification soil [32].

The uranium uptake reached the maximum at pH 3.0 and then decreased. This decrease in the adsorption of U(VI) probably reflects a reduction in the quantity of negative surface charges on the bentonite structure. Therefore, pH 3.0 was selected for further experiments.

### 3.6. The effect of initial uranium concentration

The initial U(VI) concentration was varied from 25 to 125 mg/L to evaluate its effect on adsorption efficiency. As generally expected, a change in the inlet metal ion concentration of the feed affects the adsorption. Fig. 7 illustrates the effect of initial uranium concentration on adsorption. The U(VI) adsorption increased in the initial concentration range from 25 to 100 mg/L and slightly decreased after 100 mg/L. This may be due to higher metal ion concentration enhancing the driving force to overcome mass transfer resistance between the aqueous and solid phases resulting in higher probability of collision between adsorbate molecules and adsorbent surface.

### 3.7. Effect of contact time

The effect of contact time was studied using a constant concentration of uranium solution at 30 °C. The sorption of U(VI) ions has been investigated onto adsorbed as a function of time in the range of 5–180 min. The results are shown in Fig. 8. It shows the variation of  $K_d$  and percentage adsorption with shaking time for U(VI) ions. As seen from Fig. 8, higher removal percentage of uranium is obtained

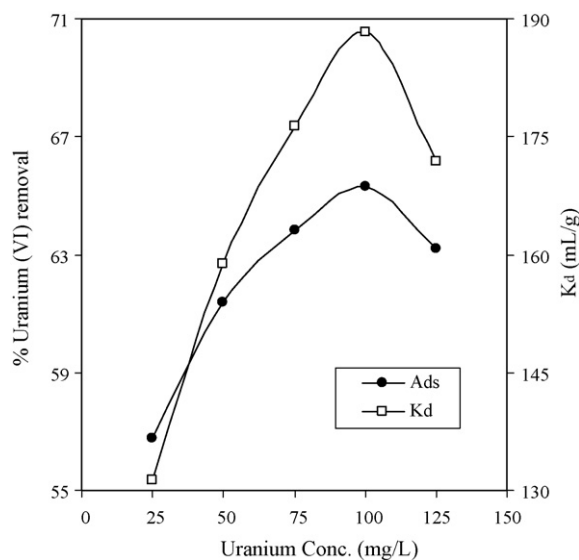


**Fig. 7.** Effect of initial U(VI) concentration (conditions: pH, 3.0; adsorbent dose, 0.1 g; contact time, 2 h; temp., 30 °C; calcination temp., 400 °C; particle size of TAB, 125 μm).

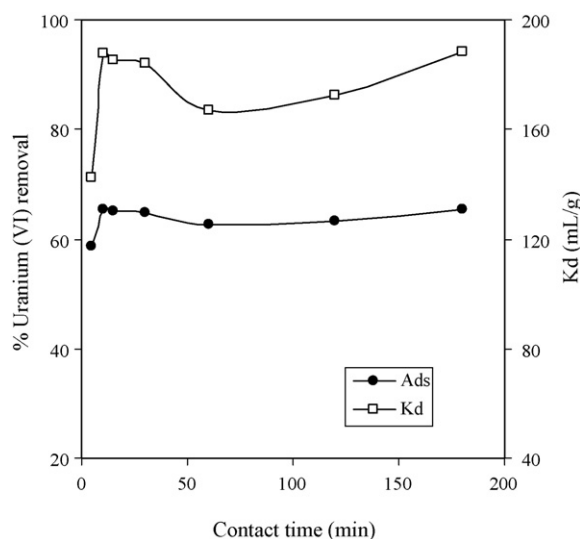


**Fig. 8.** The effect of contact time (conditions: adsorbate conc., 100 mg/L; pH, 3.0; adsorbent dose, 0.1 g; temp., 30 °C; calcination temp., 400 °C; particle size of TAB, 125 μm).

at the beginning of the adsorption. The uptake of U(VI) by TAB is very rapid, the  $K_d$  and percentage adsorption reach a maximum almost immediately after mixing of adsorbent and uranium solution, but both  $K_d$  and percentage adsorption later decrease. The initial faster rate may be due to surface adsorption and in the initial stage, the surface is free and reaction proceeds at a faster rate. Once the available free surface is clogged, then the adsorbate molecules penetrate through the pores and get adsorbed inside the pore, which is known as intra-particle diffusion. On the basis of these results 10 min shaking period was selected for all further studies.  $K_d$  and percentage sorption of uranium at the optimum adsorption conditions were found as  $196 \pm 6$  mL/g and  $66.2 \pm 0.7$ %, respectively.

### 3.8. Sorption isotherms

The adsorption isotherm indicates how the adsorption molecules distribute between the liquid phase and the solid phase

**Table 2**  
Adsorption isotherm constants for adsorption of U(VI) on TAB at 30 °C.

Freundlich isotherm constants			D–R isotherm constants			
$K_F$ (mmole g <sup>-1</sup> )	$n$	$R^2$	$\beta$ (kJ <sup>2</sup> mole <sup>-2</sup> )	$q_m$ (mmole g <sup>-1</sup> )	$E$ (kJ mole <sup>-1</sup> )	$R^2$
$3.01 \times 10^{-5}$	1.22	0.9875	$-1.024 \times 10^{-8}$	0.417	6.99	0.9903

when the adsorption process reaches an equilibrium state. The analysis of the isotherm data by fitting them to different isotherm models is an important step to find the suitable model that can be used for designing purpose. There are several isotherm equations available for analyzing experimental adsorption equilibrium data. In this study, the equilibrium experimental data for adsorbed U(VI) on TAB sample were analyzed using the Freundlich and Dubinin–Radushkevich (D–R) isotherm models. These isotherms are as follows:

(a) Freundlich isotherm model [33]:

$$\log q_e = \log K_F + \left(\frac{1}{n}\right) \log C_e \quad (3)$$

where  $K_F$  and  $n$  are Freundlich constants related to adsorption capacity and adsorption intensity, respectively.

(b) D–R isotherm model [34]:

$$\ln q_e = \ln q_m - \beta \epsilon^2 \quad (4)$$

where  $\beta$  is the activity coefficient related to mean adsorption energy (mole<sup>2</sup>/J<sup>2</sup>) and  $\epsilon$  is the Polanyi potential ( $\epsilon = RT \ln(1 + [1/C_e])$ ). The D–R isotherm is applied to the data obtained from the empirical studies. The mean adsorption energy,  $E$  (kJ mole) is as follows:

$$E = \frac{1}{\sqrt{-2\beta}} \quad (5)$$

The equilibrium data fitted to Freundlich equation (3), a fairly satisfactory empirical isotherm can be used for non-ideal adsorption. The result was represented in Table 2. From Table 2, it is noted that the values of  $n$  are bigger than 1, reflecting the beneficial adsorption. Furthermore, the value of  $K_F$  is  $3.01 \times 10^{-5}$  mmole g<sup>-1</sup> for UO<sub>2</sub><sup>2+</sup>. The numerical value of  $1/n < 1$  indicates that sorption capacity is only slightly suppressed at lower equilibrium concentration and suggests multiple binding sites, with the highest strength sites binding the sorbate first. This isotherm does not predict any saturation of the sorbent by the sorbate thus infinite surface coverage is predicted mathematically, indicating a multilayer sorption of the surface.

The sorption data have been applied to D–R model based on the heterogeneous surface of the adsorbate as in Freundlich isotherm in order to distinguish between physical and chemical adsorption. The sorption potential is independent of the temperature but varies according to the nature of sorbent and sorbate. The plot of  $\ln q_e$  vs.  $\epsilon^2$  as shown in Fig. 9 is a straight line. From the slope and intercept of this plot the values of  $\beta = -1.024 \times 10^{-8}$  kJ<sup>2</sup> mole<sup>-2</sup> and  $q_m = 0.417$  mmole UO<sub>2</sub><sup>2+</sup>/g have been estimated. The mean sorption energy ( $E$ ) is given by Eq. (5). The numerical value of mean sorption energy is in the range of 1–8 and 9–16 kJ mole<sup>-1</sup> forecast the physical adsorption and chemical adsorption, respectively [35]. The value of  $E$  is expected for physical adsorption. The D–R model was found to fit the test data better than the Freundlich model.

### 3.9. Thermodynamic studies

This adsorption potential is independent of the temperature, but it varies depending on the nature of adsorbent and adsorbate. Using the following equations, the thermodynamic parameters of

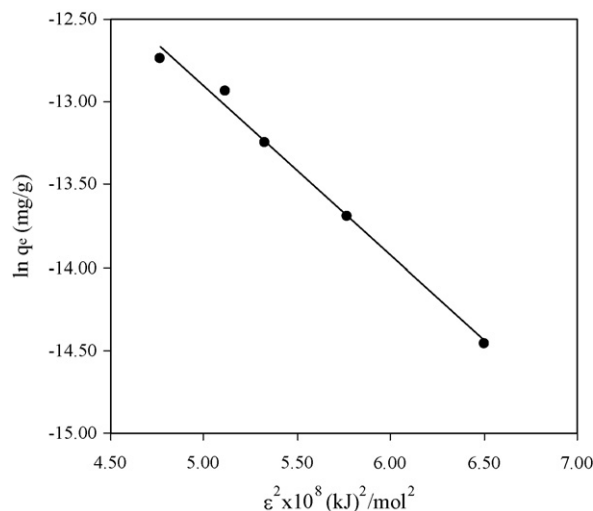


**Fig. 9.** Dubinin–Radushkevich (D–R) sorption isotherm of uranium onto TAB.

the adsorption process can be determined from the experimental data:

$$\ln K_d = \frac{\Delta S}{R} - \frac{\Delta H}{RT} \quad (6)$$

$$\Delta G = \Delta H - T\Delta S \quad (7)$$

$$K_d = \frac{q_e}{C_e} \quad (8)$$

where  $K_d$  is the distribution coefficient for the adsorption,  $\Delta S$ ,  $\Delta H$  and  $\Delta G$  are the changes of entropy, enthalpy and the Gibbs energy,  $q_e$  is the equilibrium concentration of U(VI) on the adsorbent (mg/g),  $T$  (K) is the temperature,  $R$  (J mole<sup>-1</sup> K<sup>-1</sup>) is the gas constant. The values of  $\Delta H$  and  $\Delta S$  were determined from the slopes and intercepts of the plots of  $\ln K_d$  vs.  $1/T$ .

The influence of temperature variation was examined on the sorption of U(VI) on TAB from 1 M HNO<sub>3</sub> solution using 10 min equilibration time and 25 mg TAB/50 mL of sorptive solution from 293 to 333 K. Thermodynamic parameters were calculated for this system by using the following Eq. (6) and (7). The plot of  $\ln K_d$  against  $1/T$  for U(VI) is shown in Fig. 10. The values of enthalpy and entropy were obtained from the slope and intercept of  $\ln K_d$  vs.  $1/T$  plots, which were calculated by a curve-fitting program. Gibbs free energy was calculated by using the following well-known Eq. (8).

The values of the thermodynamic parameters for the sorption of U(VI) on TAB are given in Table 3. The negative values for the Gibbs free energy change,  $\Delta G$ , show that the adsorption process for the TAB is spontaneous and the degree of spontaneity of the reaction increases with increasing temperature. The increase in adsorption with temperature may be attributed to either increase in the number of active surface sites available for adsorption on the adsorbent or the desolvation of the adsorbing species and the decrease in the thickness of the boundary layer surrounding the adsorbent with temperature, so that the mass transfer resistance of adsorbate in the boundary layer decreases. The positive value of enthalpy change,  $\Delta H$ , show the adsorption of uranium is endothermic. Also the positive entropy favors complexation and stability of sorption.

**Table 3**  
Thermodynamic parameters for the adsorption of uranium onto TAB.

$\Delta H^\circ$ (kJ mole <sup>-1</sup> )	$\Delta S^\circ$ (kJ mole <sup>-1</sup> K <sup>-1</sup> )	$\Delta G^\circ$ (kJ mole)				
		293 K	303 K	313 K	323 K	333 K
0.0193	0.108	-31.67	-32.75	-33.83	-34.92	-35.99

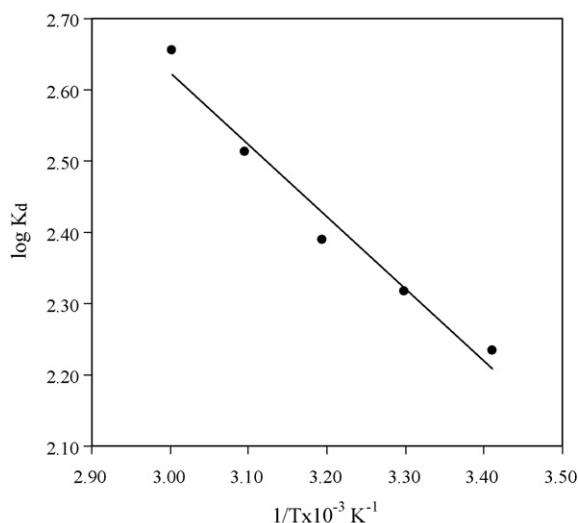


**Fig. 10.** Influence of temperature on the thermodynamic behavior of adsorption of uranium onto TAB.

### 3.10. Desorption of adsorbed uranium from the TAB

Desorption process was carried out as a function some parameters such as the kind of desorptive solution, concentration of desorptive solution, contact time and number of desorption stage. The uranium concentration in the solution after desorption process was determined using TOPO-DBM method.

After adsorption of uranium onto TAB, TAB was treated with different desorptive solutions to recover the adsorbed uranium from TAB. Desorption of uranium from loaded TAB studied as a function some parameters such as the kind of desorptive solution, concentration of desorptive solution, contact time and stage of desorption. Desorption yields were shown in Table 4. TAB showed the lower desorption yield using NaNO<sub>3</sub>, H<sub>2</sub>SO<sub>4</sub>, NaCl, and H<sub>2</sub>O compared to the other desorptive solutions. 1 M HNO<sub>3</sub> and 1 M CH<sub>3</sub>COONH<sub>4</sub> represents relatively high desorption yield for uranium. Other desorption parameters were changed to increase the desorption yield.

The effect of concentration of HNO<sub>3</sub> solution on desorption of uranium from TAB showed that 1 M HNO<sub>3</sub> solution has a maximum yield (94.6%). Desorption of uranium from adsorbent was reached to maximum value in a period of less than 30 min. Desorption tests showed that uranium could be quantitatively desorbed with 1 M HNO<sub>3</sub> at 30 °C in one stage.

**Table 4**  
Desorption yields of some desorptive solutions.

Elution solution	Desorption (%)	Elution solution	Desorption (%)
1 M CH <sub>3</sub> COONH <sub>4</sub>	91.10	1 M EDTA	60.25
1 M NaNO <sub>3</sub>	4.70	1 M H <sub>2</sub> SO <sub>4</sub>	21.00
1 M NaCl	5.90	1 M NaOH	65.92
1 M Na <sub>2</sub> CO <sub>3</sub>	70.60	1 M HNO <sub>3</sub>	94.60
1 M NaHCO <sub>3</sub>	80.22	H <sub>2</sub> O	5.00
1 M HCl	75.62		

## 4. Conclusions

Natural clays present a major advantage of giving low cost recovery processes making them suitable for use in water purification. Moreover, their regeneration does not present any problem and, when needed, the recovering of the fixed element could be reached even by leaching the loaded material.

The results of this study indicate that TAB can be successfully used for the recovery of hexavalent uranium from aqueous solutions under the optimized conditions. Bentonites are an effective adsorbent for the recovery uranium from aqueous solution. Bentonite is cheap and found at several localities in Turkey. Taking into account the results, we have considered it of great interest to assess the ability of locally available bentonite for the adsorption of U(VI) from aqueous solutions.

The adsorption of uranium onto TAB follows Freundlich and D–R isotherms. In the adsorption systems,  $n$  value is  $n > 1$  which indicates that adsorption intensity is favorable over the entire range of concentrations studied. The  $K_F$  value of the Freundlich equation also indicates that TAB has a very high adsorption capacity for U(VI) ions in aqueous solutions.

The temperature variations have been used to evaluate the values of  $\Delta H$ ,  $\Delta S$  and  $\Delta G$ . The negative value of  $\Delta G$  showed spontaneous nature of adsorption. The positive value of  $\Delta H$  indicates the endothermic behavior of the adsorption reaction of U(VI) ions and suggests that a large amount of heat is consumed to transfer the U(VI) ions from aqueous into the solid phase.

The transition metal ions must give up a larger share of their hydration water before they could enter the smaller cavities. Such a release of water from the divalent cations would result in positive values of  $\Delta S$ . This mechanism of the adsorption of U(VI) ions is also supported by the positive values of  $\Delta S$ , which show that U(VI) ions are less hydrated in the TAB layers than in the aqueous solution. Also, the positive value of  $\Delta S$  indicates the increased disorder in the system with changes in the hydration of the adsorbing U(VI) cations. The value of sorption energy gives an indication about the nature of sorption.

The experimental results show that 1 M HNO<sub>3</sub> is a successful solution for desorption of uranium.

## References

- [1] Z. Ding, R.L. Frost, Study of copper adsorption on montmorillonites using thermal analysis methods, *J. Colloid Interface Sci.* 269 (2004) 296–302.
- [2] S.E. Bailey, T.J. Olin, R.M. Bricka, D.D. Adrian, A review of potentially low-cost sorbents for heavy metals, *Water Res.* 33 (1999) 2469–2479.
- [3] A.M.M. Khraisheh, Y.S. Al-degs, W.A.M. McMinn, Remediation of wastewater containing heavy metals using raw and modified diatomite, *Chem. Eng. J.* 19 (2004) 177–184.
- [4] J.C. Echeverría, E. Churio, J.J. Garrido, Retention mechanism of Cd on illite, *Clay Clay Miner.* 50 (2002) 614–623.
- [5] R. Donat, A. Akdogan, E. Erdem, H. Cetisli, Thermodynamics of Pb<sup>2+</sup> and Ni<sup>2+</sup> adsorption onto natural bentonite from aqueous solutions, *J. Colloid Interface Sci.* 286 (2005) 43–52.
- [6] J.H. Potgieter, S.S. Potgieter-Vermaak, P.D. Kalibantonga, Heavy metals removal from solution by palygorskite clay, *Miner. Eng.* 19 (2006) 463–470.
- [7] W. Wu, Q. Fan, J. Xu, Z. Niu, S. Lu, Sorption–desorption of Th(IV) on attapulgite: effects of pH, ionic strength and temperature, *Appl. Radiat. Isot.* 65 (2007) 1108–1114.
- [8] M.F. Brigatti, C. Lugli, L. Poppi, Kinetics of heavy-metal removal and recovery in sepiolite, *Appl. Clay Sci.* 16 (2000) 45–57.
- [9] G.E. Christids, P.W. Scott, A.C. Dunham, Acid activation and bleaching capacity of bentonites from the islands of Milos and Chios, Aegean, Greece, *Appl. Clay Sci.* 12 (1997) 329–347.

- [10] S. Kozar, H. Bilinski, M. Branica, M. Schwugar, Adsorption of Cd(II) and Pb(II) on bentonite under estuarine and seawater conditions, *J. Sci. Total Environ.* 121 (1992) 203–216.
- [11] M.T. Olguin, M.S. Rios, D. Acosta, P. Bosch, S. Bulbulian,  $UO_2^{2+}$  sorption on bentonite, *J. Radional. Nucl. Chem.* 218 (1997) 65–69.
- [12] A.J. Dent, J.D.F. Ramsay, S.W. Swanton, An EXAFS Study of uranyl ion in solution and sorbed onto silica and montmorillonite clay colloids, *J. Colloid Interface Sci.* 150 (1992) 45–60.
- [13] H.C.H. Darley, G.R. Gray, Composition and Properties of Drilling and Completion Fluids, 5th ed., Gulf Publ. Co., TX, USA, 1988.
- [14] F. Kooli, W. Jones, Characterization and catalytic properties of a saponite clay modified by acid activation, *Clay Miner.* 32 (1997) 633–643.
- [15] I.E. Odom, Smectite clay minerals: properties and uses, *Philos. Trans. R. Soc. Lond., Series A* 311 (1984) 391–409.
- [16] K. Emmerich, Spontaneous rehydroxylation of a dehydroxylated cis-vacant montmorillonite, *Clay Clay Miner.* 48 (2000) 405–408.
- [17] D.R. Corbin, B.F. Burgess, A.J. Vega, R.D. Farlee, Comparison of analytical techniques for the determination of silicon and aluminum content in zeolites, *Anal. Chem.* 59 (1987) 2722–2728.
- [18] N. Kabay, Modifiye Edilmiş Polimerik Amidoksim Reçinelerin Deniz Suyundan Uranyum Kazanımına Uygulanabilirliğinin İncelenmesi, E.Ü. Araştırma Fonu Projesi, NBE 003, 1994 (in Turkish).
- [19] C.A. Francois, Rapid spectrophotometric determination of submilligram quantities of uranium, *Anal. Chem.* 30 (1958) 50–54.
- [20] W.M. Tuddenham, R.J.P. Lyon, Infrared techniques in the identification and measurement of minerals, *Anal. Chem.* 32 (1960) 1630–1634.
- [21] V.A. Drits, G. Besson, F. Muller, An improved model for structural transformations of heat-treated aluminous dioctahedral 2:1 layer silicates, *Clay Clay Miner.* 43 (1995) 718–731.
- [22] S.K. Srivastava, R. Tyagi, N. Pant, N. Pal, Studies on the removal of some toxic metal ions. Part II. Removal of lead and cadmium by montmorillonite and kaolinite, *Environ. Technol. (Lett.)* 10 (1989) 275–282.
- [23] V.S. Komarov, I.B. Dubnitskaya, Physicochemical Groundings in the Regulation of Porous Structure of Adsorbents and Catalysts, Science and Technics, Minsk, 1981, pp. 35–38.
- [24] E.A. Gerasimov, S.J. Bachvarov, Technology of Ceramic Products, Technics, Sofia, 1977, pp. 98–105.
- [25] R. Stefanova, S. Dimitrova, B. Balushev, St. Boyadjieva, Municipal and rural water supply and water quality, in: *Proc. Int. Conf. Poznan Poland, 2, 1996*, pp. 321–328.
- [26] M. Chorom, P. Rengasamy, Effect of heating on swelling and dispersion of different cationic forms of a smectite, *Clay Clay Miner.* 44 (1996) 783–790.
- [27] B. Ritherdon, C.R. Hughes, C.D. Curtis, F.R. Livens, J. Fred, W. Mosselmans, S. Richardson, A. Braithwaite, Heat-induced changes in speciation and extraction of uranium associated with sheet silicate minerals, *Appl. Geochem.* 18 (2003) 1121–1135.
- [28] L. Heller-Kallai, I. Rozenson, Dehydroxylation of dioctahedral phyllosilicates, *Clay Clay Miner.* 28 (1980) 355–368.
- [29] T.J. Sorg, Removal of uranium from drinking water by conventional treatment methods, in: Cothorn, Rebers (Eds.), *Radon, Radium and Uranium in Drinking Water*, Lewis Publishers, Michigan, 1991, p. 173, ISBN: 0 87371 2.
- [30] J.M. Zachara, J.P. McKinley, Influence of hydrolysis on the sorption of metal cations by smectites; importance of edge coordination reactions, *Aquat. Sci.* 55 (1993) 250–261.
- [31] A.M.L. Kraepiel, K. Keller, F.M.M. Morel, A model for metal adsorption on montmorillonite, *J. Colloid Interface Sci.* 210 (1999) 43–54.
- [32] B. Batchelor, Leach models for contaminants immobilized by pH-dependent mechanisms, *Environ. Sci. Technol.* 32 (1998) 1721–1726.
- [33] H.M.F. Freundlich, Over the adsorption in solution, *J. Phys. Chem.* 57 (1906) 385–470.
- [34] M.M. Dubinin, L.V. Raduskhevich, Equation of the characteristic curve of activated charcoal, *Proc. Acad. Sci. U.S.S.R.* 55 (1947) 331–333.
- [35] M.M. Saeed, Adsorption profile and thermodynamic parameters of the preconcentration of Eu(III) on 2-thenoyltrifluoroacetone loaded polyurethane (PUR) foam, *J. Radioanal. Nucl. Chem.* 256 (2003) 73–80.